

TA7

CG

CER 68/69-44

COPY 2

REPORT ON BALLOON SHELTER TESTS

by

Erich J. Plate

Professor, Colorado State University

March 1969

**REPORT ON BALLOON SHELTER TESTS**

**prepared by**

**Erich J. Plate**

**Professor of Civil Engineering .**

**Colorado State University**

**for**

**National Center of Atmospheric**

**Research**

**March 1969**

**submitted by**

*Erich Plate*

## BALLOON SHELTER TESTS

During the year 1968 experiments were performed in the wind tunnels of the Fluid Dynamics and Diffusion Laboratory, Colorado State University on possible shelters for meteorological balloons. Two basic shapes were tested, one consisting of a square plate set perpendicular to the wind, and the second one a wedge-type of same height and projection on the plane normal to the flow, with an apex angle of  $90^\circ$ . The models consisted of steel frames over which the screen materials has been stretched, as shown in Fig. 1. They were designed into sharp outer edges, so that separation would always occur at the edges. Two different screen materials were tested: ordinary bug screen and a special fiberglass material provided by NCAR. Samples of both materials are attached to this report.

### 1. General considerations

In some earlier work (Plate and Lin (1965) "The velocity field downstream from a two-dimensional model hill") it is shown that modeling of a field situation in a laboratory is accomplished if  $C_D$  (i.e., the drag coefficient of the shelter) and the ratio  $h/\delta$  are the same in both field and laboratory, where the length  $h$  is the structure height and  $\delta$  is the thickness of the boundary layer. Although these requirements were for two-dimensional flow fields, it can be expected that only minor modification would be required for the three-dimensional counterpart.

### 1.1 The drag coefficient $C_D$ for solid shelters

Constant drag coefficients  $C_D$  can be obtained approximately by having sharp edges of the shelters both in model and prototype. Then the drag coefficient defined by

$$C_D = \frac{D}{\frac{1}{2} \rho u_\infty^2 h \cdot w} \quad (1)$$

where  $D$  is the drag on the shelter, becomes independent of the Reynolds number  $u_\infty h/\nu$ . In this equation,  $h$  is the height and  $w$  the breadth of the projection of the shelter on a plane perpendicular to the direction of the ambient air flow  $u_\infty$  (at some reference height). Ordinarily  $C_D$  would be a function of Reynolds number. However, by sharpening the edges of the shelter, the separation line of the boundary layer on the shelter becomes fixed, resulting in a  $C_D$  which is independent of the Reynolds number. It does, however, depend slightly on  $h/\delta$ , but this dependency is not critical and can be taken care of by making the boundary layer of the approach flow as thick as possible.

The drag coefficient not only determines the drag on the shelter but also the shape of the flow field downstream from the shelter. In general, the larger  $C_D$ , the larger will be the sheltered area, but evidently at the price of a larger drag force, as well as higher turbulence levels.

For a solid screen, or a square flat plate, it is possible to obtain the drag coefficient, to a first approximation, from the relation:

$$\frac{C_D \text{ infinite plate}}{C_D \text{ rectangular plate}} \left| \begin{array}{l} \text{in free stream} \\ \text{in boundary layer} \end{array} \right. \quad (2)$$

or (see Rouse (1950), p. 126, for free stream ratio)

$$\frac{1.90}{1.16} = \frac{0.8}{C_D} \quad (3)$$

when the value of 0.8 for the drag coefficient of the infinite plate in a boundary layer has been taken from experimental results of Plate (1964). Consequently:

$$C_D = \frac{1.16}{1.90} \cdot 0.8 = 0.5 \quad (4)$$

to a first approximation.

Some measurements of Vichery (1968) for a plate which was neither fully in the free stream nor on a floor were found to yield  $C_D = 1.0$ , approximately, which falls between the assumed free stream value of 1.16 and the calculated boundary layer value of 0.5. A safe value, to be used in calculation, might therefore be taken as about  $C_D = 0.7$ .

In the quoted paper, Vichery also points out that in addition to the mean drag, there also occurs a fluctuating drag whose RMS - value might be as much as 10% of the mean. He does not give a peak value, but a suitable safety factor should be used. In view of the fact that the structure of the shelter will be very light, a safety factor of at least two is recommended, i.e., for the design of the structure,  $C_D = 1.0 - 1.2$  should be used.

## 1.2 The drag coefficient $C_D$ for porous shelters

It is very likely that the effect of porosity is also a Reynolds number effect, but this time the Reynolds number should be based on the properties of the screen material. Since air flow and viscosity in model and prototype are the same, it is required that the screens are the same also, to meet Reynolds number similarity. Actually, however, it is found that for a given screen material the aerodynamic behavior is practically independent of Reynolds number. A measure of the aerodynamic behavior can be obtained by determining the pressure drop  $\Delta p$  across a screen which passes a velocity of  $\bar{u}$  fps. The pressure drop coefficient

$$c_p = \frac{\Delta p}{\frac{1}{2} \rho \bar{u}^2} \quad (5)$$

should become independent of the Reynolds number.

For a porous screen, the pressure drop coefficient yields a measure of the force exerted on the screen. Let  $\bar{u}$  be the velocity observed, in the model case directly downstream of the screen. Then, to a rough approximation:

$$D = c_p \frac{1}{2} \rho \bar{u}^2 \cdot w \cdot h \quad (6)$$

or, if the reduction factor  $c$  is introduced:

$$c = \frac{\bar{u}}{u_\infty} \quad (7)$$

which signifies the reduction of velocity obtained by a screen, then:

$$D = c_p c^2 \cdot \frac{1}{\rho_2} \rho u_\infty^2 w \cdot h \quad (8)$$

For a given screen material and shelter shape, the coefficients  $c_p$  and  $c$  are found from wind tunnel experiments.

Comparison of Eqs. 1 and 8 shows that for a porous screen we have:

$$C_D = c_p c^2 . \quad (9)$$

The experiments show that for a porous screen, both  $c$  and  $c_p$  are approximately independent of velocity, so that  $C_D$  is found independent of Reynolds number for porous screens also--provided that the screens are the same in model and prototype.

For the bug screen material used, we find a value of  $c_p = 0.62$  and a reduction factor  $c = 0.5$ . Consequently, the equivalent drag coefficient, according to Eq. 9 is

$$C_D = 0.62 \cdot \frac{1}{4} = 0.16 .$$

It goes without saying that the relation EQ. 9 is valid only for  $C_D < 0.5 \div 0.7$ . Once  $C_D = 0.5 \div 0.7$  is reached, a screen behaves like a solid screen regardless of its actual porosity.

### 1.3 The effect of $h/\delta$

The parameter  $h/\delta$  determines mainly the velocity distribution downstream of the shelter, outside the sheltered region. For the sheltered region its effect is mainly on the drag coefficient.  $C_D$  varies, for thick boundary layers,

approximately proportional to  $(h/\delta)^{2/7}$  in the case of an infinitely wide shelter. For a finite width shelter, the effect should be even smaller, and thus, if we just make the profile approaching the shelter roughly logarithmic and as thick as possible, the values of  $C_D$  obtained in the experiments should be transferable without much error to the atmospheric conditions, which leads to the proposed value of  $C_D \approx 0.5 \div 0.7$ .

#### 1.4 Pulsating forces on the balloon.

A sharp edged device like the balloon shelter model is very likely to shed regular eddies, (of Karman type vortices) which will be the dominant feature in the large scale turbulence. Unfortunately, for the experimental results of this preliminary study, no satisfactory measurements of the eddy shedding velocities were obtained. It can, however, be expected that the frequency  $f$  of the dominant eddies is given approximately by the Strouhal frequency obtained from the relation

$$St = \frac{fW}{u_\infty} = 0.08 \text{ to } 0.11$$

where  $St$  is the Strouhal number, which according to results of Vichery (1968) is approximately constant and lies within the indicated range, and  $f$  is the peak frequency. Typically, for a shelter of 70 ft. width, one would expect a dominant frequency of about (at 30 ft/sec)

$$0.1 \cdot \frac{30}{70} \quad f \approx \frac{30}{70} = \frac{0.045 \text{ Hz}}{0.45 \text{ Hz}}$$



More accurate results should be obtained in the testing program for the final design.

## 2. Experimental data and results

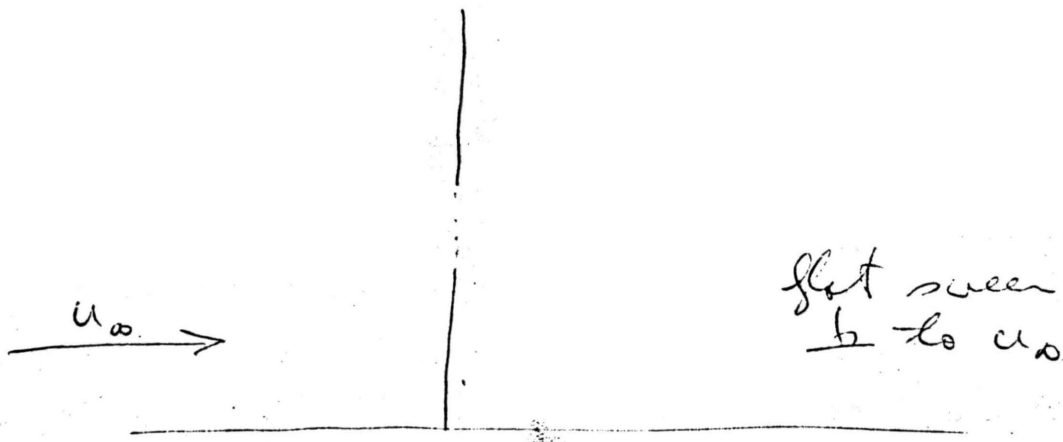
### 2.1 Velocity distributions

Vertical distributions of horizontal mean velocities were taken to map out the sheltered region. They were taken at distances of 3" (=  $1/4 w$ ), 6", 12" and 18" downstream from the shelter models, with a lateral distance  $y$  from the centerline of from 0 to 12". The profiles of the approach velocity for the shelters are shown in Fig. 2. All other profiles are filed in the data files of CSU. From the profiles, isotachs were constructed which are shown in Figs. 3 to 13. Two types of figures are shown. Profiles along the centerline, to show the reduction of wind velocity in a plane along the center at different velocities, are given in Figs. 3, 5, 6, 8, 9-3, 11, and 12-3. Note that downwind distances from the wedge are measured from the downwind edges of the model. The remainder of the isotach figures show cross sections through the sheltered regions. Only half of the sheltered region is shown, since the (vertical) z-axis is an axis of symmetry.

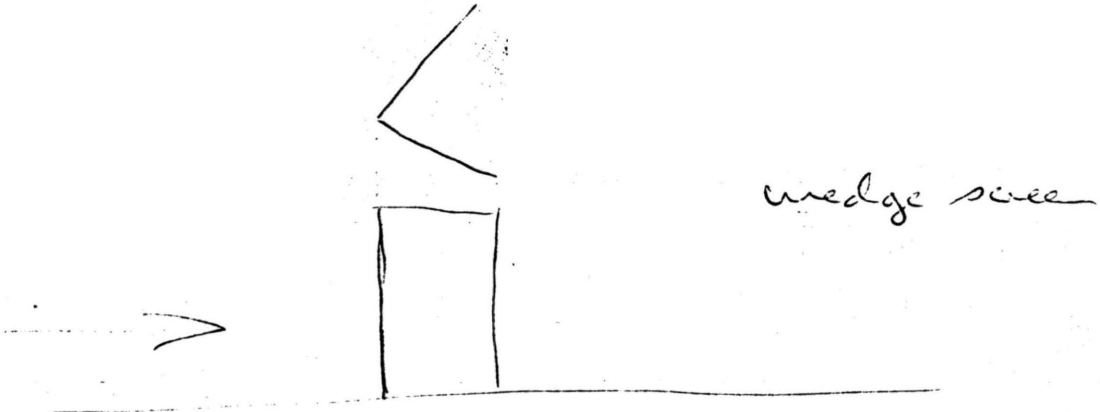
### 2.2 Turbulence data

We took two types of turbulence data: turbulence recordings at a distance of 3" from the centerline at four different downstream distances of the NCAR screen square plate and wedge, at one height of 6" (=  $1/2 h$ ) above the

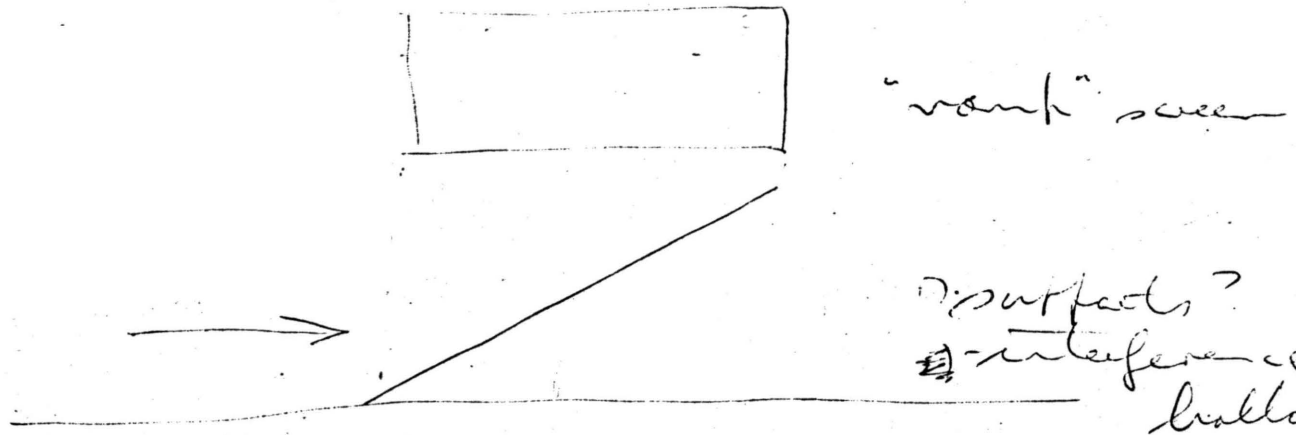
lvs.  
12/9/69.



flat sweep  
to  $u_\infty$



wedge sweep



"ramp" sweep

- 1) supports?
- 2) interference with balloon
- 3) wing tip vortices? of delta wing
- 4) rigidity? of  $C_h$ .

floor. These data, recorded on strip charting give an indication of the low frequency turbulence which is likely to effect the balloons. However, we cannot detect any low frequency component in the recordings which might be significant. We feel that this result is due to the fact that eddy shedding will be most pronounced at the edges of the screens, where measurements were not taken. At this time, it is therefore only possible to use the quoted results by Vichery as a rough guide, and to prepare a more extensive record of the turbulence, at the edges of the screen, during tests on the final design.

The second set of turbulence data was on the turbulent intensity  $\overline{u'^2}$  when  $u'$  is the fluctuating velocity component (with time mean zero) in the direction of the mean local flow velocity. The overbar denotes the time mean. Due to the limitations of our RMS-Analyzers, these data are of frequencies higher than 2 cps, they are thus not representative of the low frequency end of the spectrum, which is of greatest importance for balloon sheltering. Profiles of  $\overline{u'^2}$  along a distance  $1/4 w$  off the centerline are shown in Fig. 14.

### 2.3 Pressure drop coefficients

Pressure drop coefficients  $c_p$  were obtained by stretching screens across the whole cross section of the wind tunnel and measuring velocity and pressure drop across the screen with two pitot-static tubes located one upstream and one downstream of the screen. For the NCAR screen we

found a pressure drop coefficient  $c_p$  of 22--implying an almost solid screen--independent of Re number. For the bug screen, the pressure drop coefficient was found to be 0.62. Again, all Reynolds number dependencies, if existing, were hidden in the scatter of the experimental results.

### 3. Conclusions

On the basis of the reported experiments, the following conclusions on the design of a balloon shelter are drawn.

1. Porous shelter surfaces, as compared to solid (or almost solid surfaces) have a considerably lower turbulence level associated with them, but a mean velocity level which is higher in the sheltered region. Furthermore, the forces on a porous screen are much smaller. A rough estimate gave drag coefficients for the square plate data of 0.5 to 0.7 and 0.16 for solid and bug screen surfaces, respectively.

2. A square plate shelter provides a larger sheltered area, but much larger low frequency turbulence than a wedge shaped design. On this basis, and on the basis of construction convenience, it is recommended that the wedge be used, in a suitable modification to meet structural requirements.

3. The average reduction in mean wind speed effected by the porous screen tested (bug screen) was 50 percent at all velocities. Neither the flow pattern nor the percentage reductions attained depended on the ambient velocity  $U_\infty$ . Consequently, it is felt that prototype screen and model screens should be the same. It is recommended that a material should be used for the screens which is slightly

denser than the bug screen, such as a double layer of bug screen or equivalent.

4. Finally, it is recommended that on the basis of these findings the desired shelter should be engineered to fit suitably into the sheltered areas indicated in Figs. 3 to 13. The final design should then be modeled and wind tunnel tests be performed to check its actual characteristics.

Erich J. Plate  
Professor of Civil Engineering  
Colorado State University  
March 1969

## REFERENCES

- Plate, E. and C. Y. Lin (1965), "The velocity field downstream from a two-dimensional model hill." Final Report, Part I, U.S. Army Materiel Agency, Contract DA-AMC-36-039-63-G7.
- Rouse, H. (1950), editor, "Engineering Hydraulics." J. Wiley, New York.
- Plate, E. (1964), "The drag on a smooth flat plate with a fence immersed in its turbulent boundary layer," ASME paper No. 64 FE-17.
- Vichery, B.J. (1968), "Load fluctuations in turbulent flow." Proc. ASCE, Journal Engr. Mech. Division, Vol. 94, paper No. EM1.

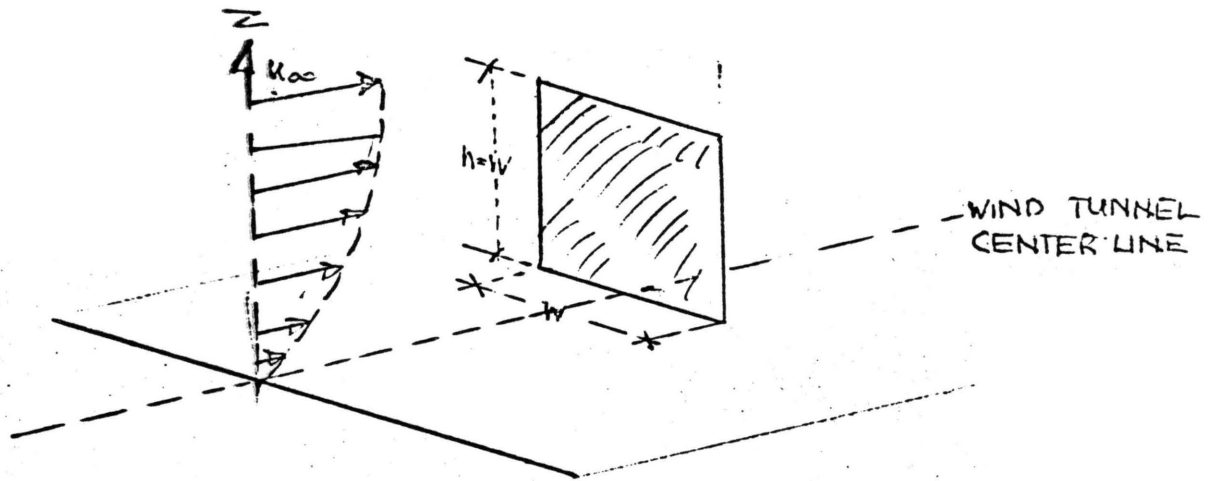


FIG 1A SCHEMATIC OF SQUARE SCREEN

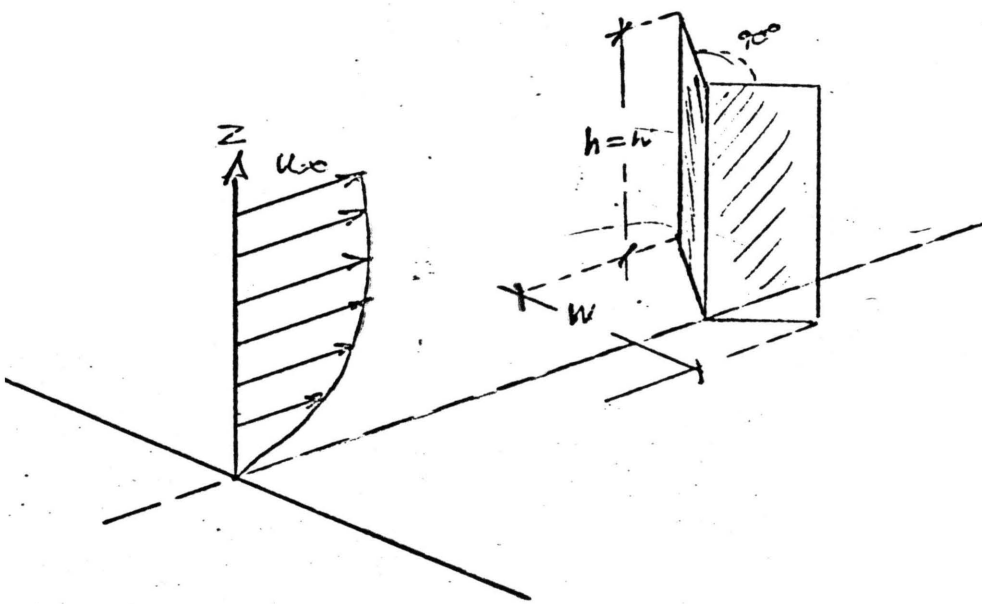


FIG 1B SCHEMATIC VIEW OF WEDGE SCREEN

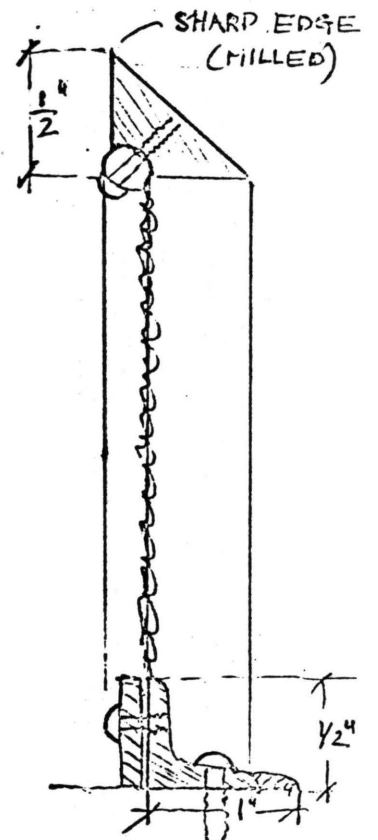


FIG 1C CONSTRUCTION DETAILS (NOT TO SCALE)

FIG 1: SCREEN MODELS

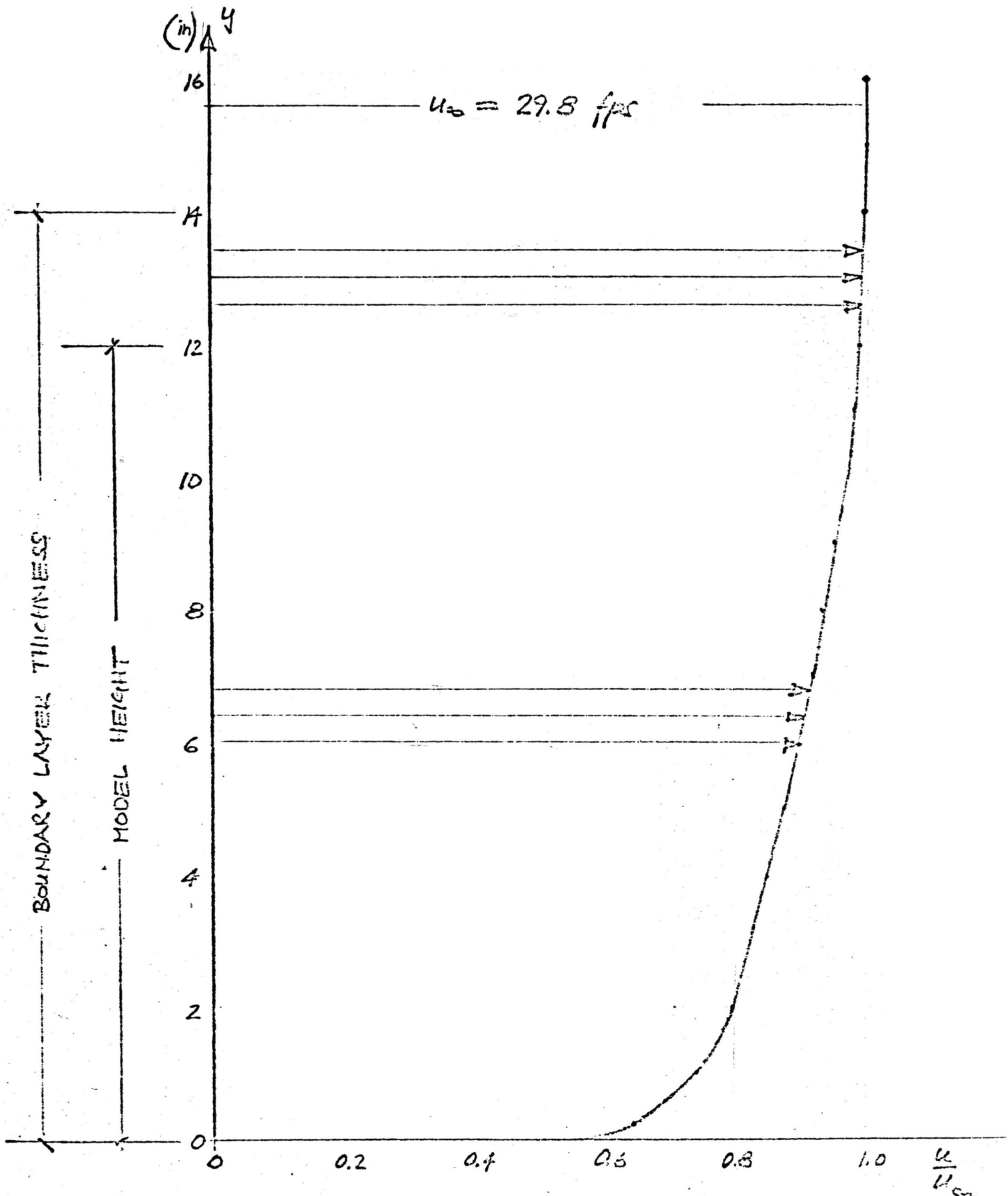
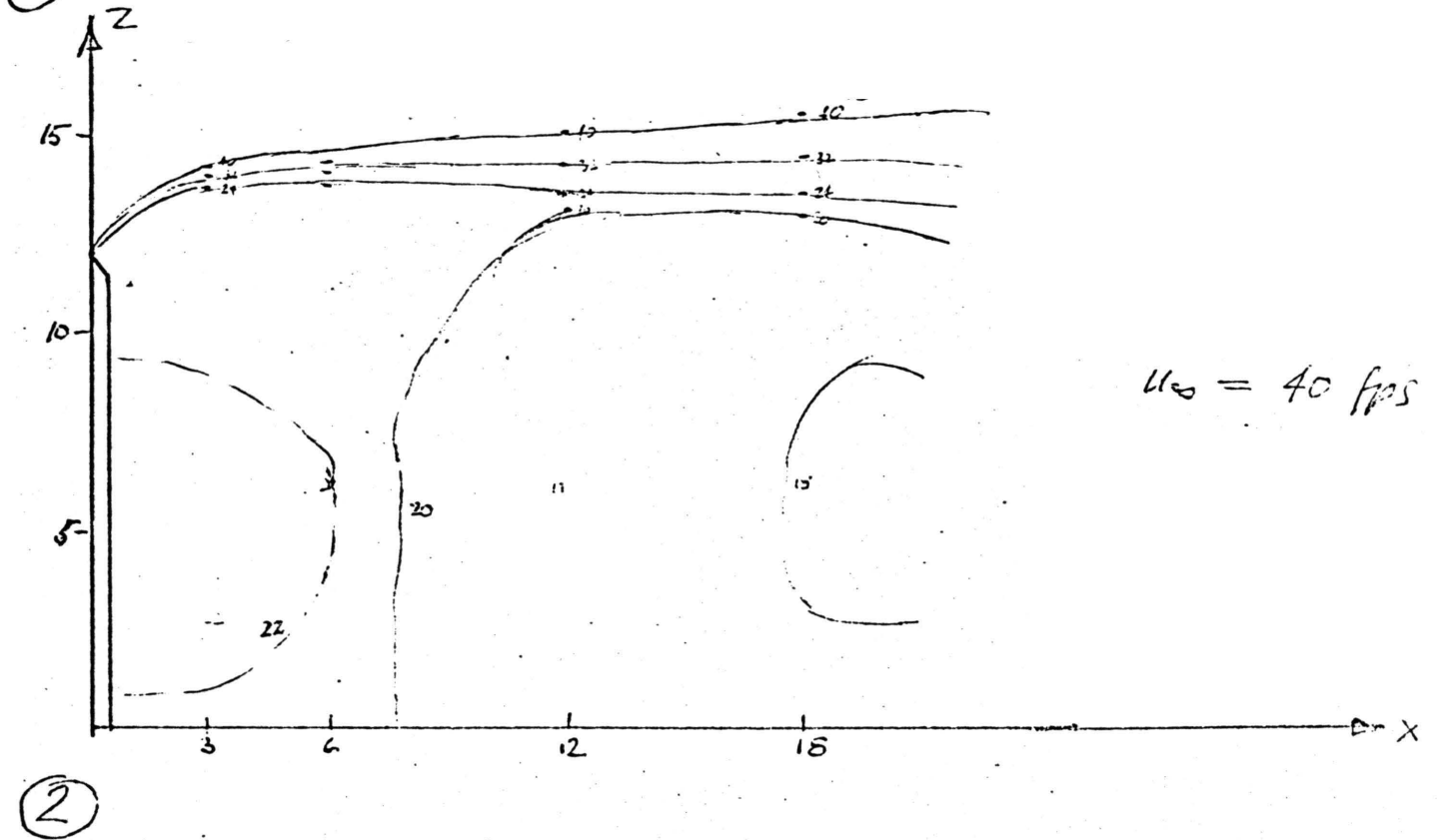
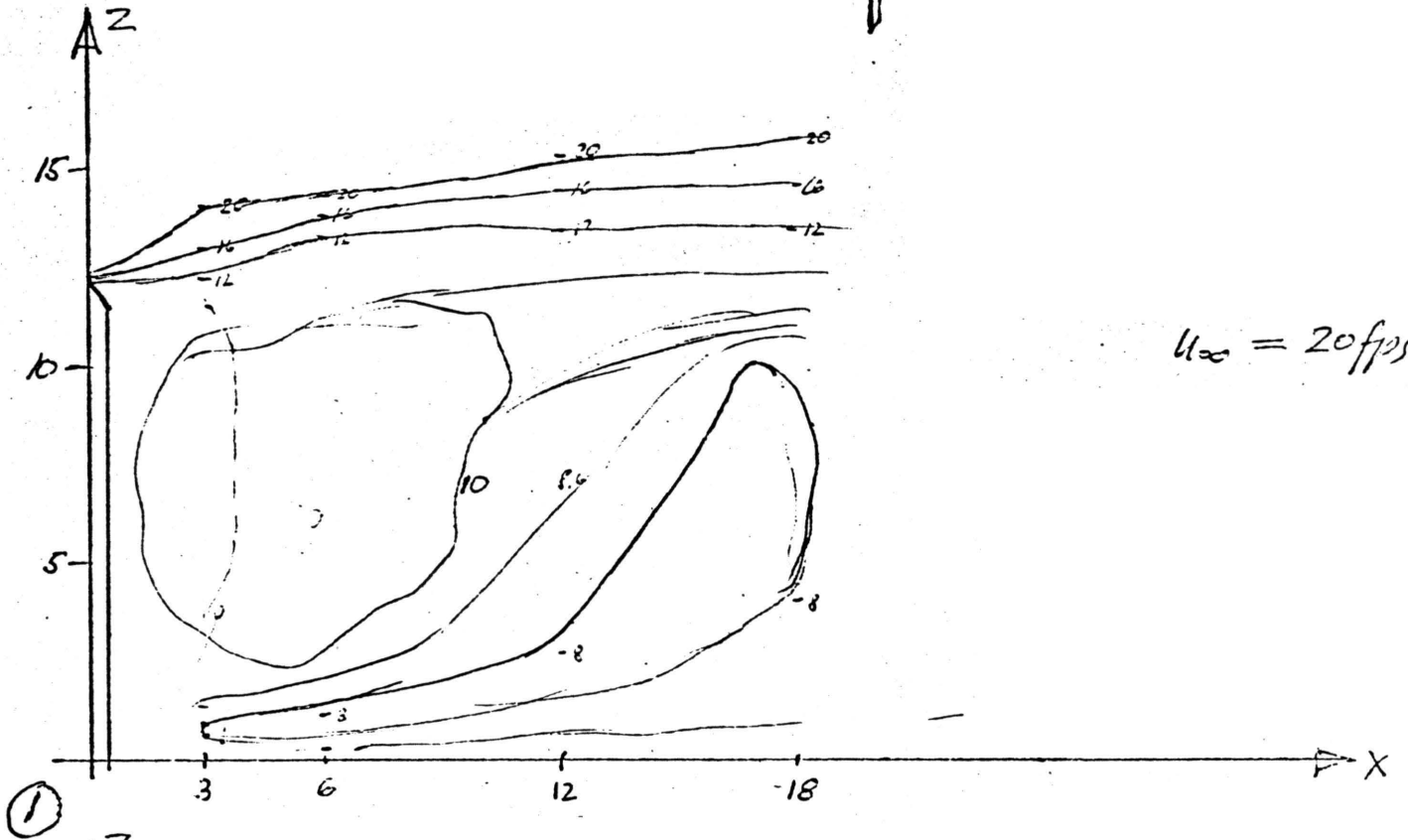
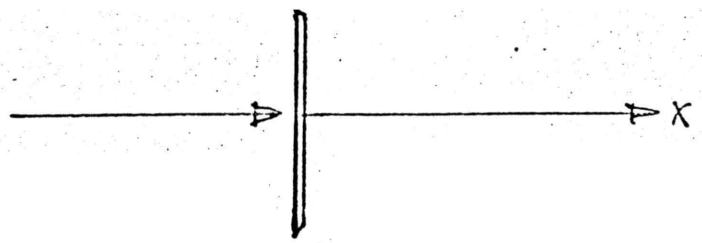


FIG 2 : APPROACH WIND PROFILE  
(at  $x = 5W$  upstream of model)



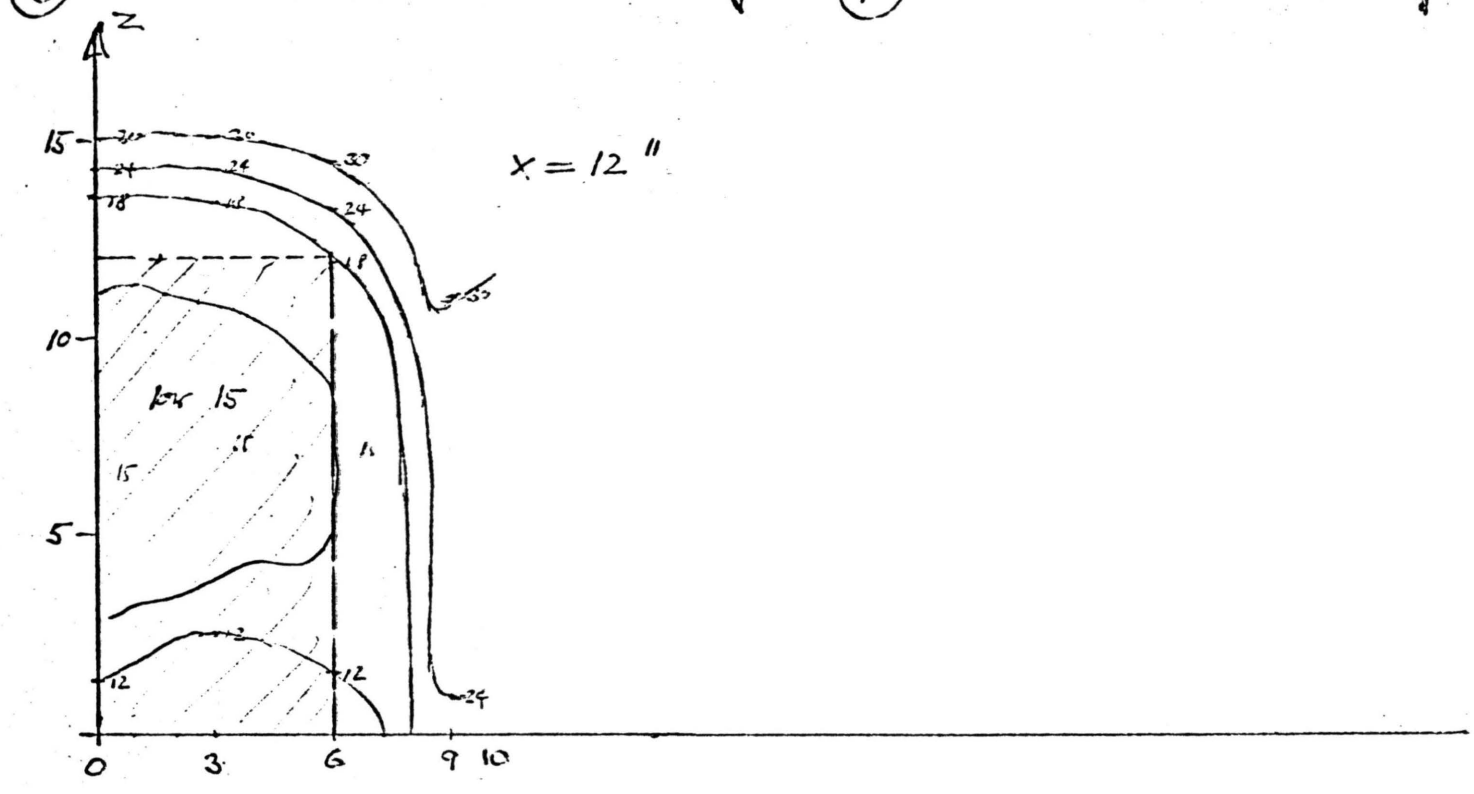
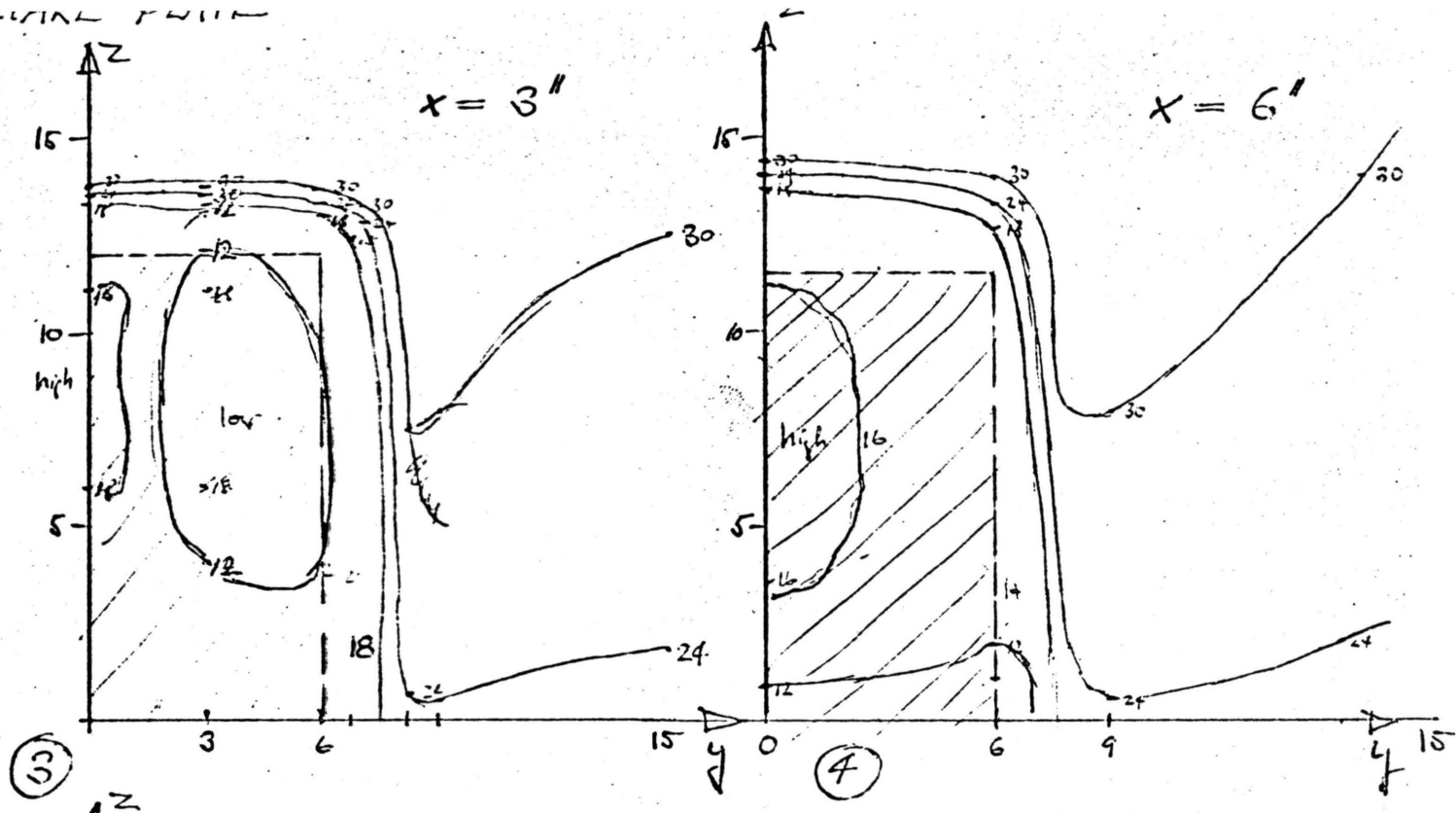
BUG SCREEN  
SQUARE PLATE



VELOCITY AT  $y=0$  ( $\phi$ )

Fig. 3

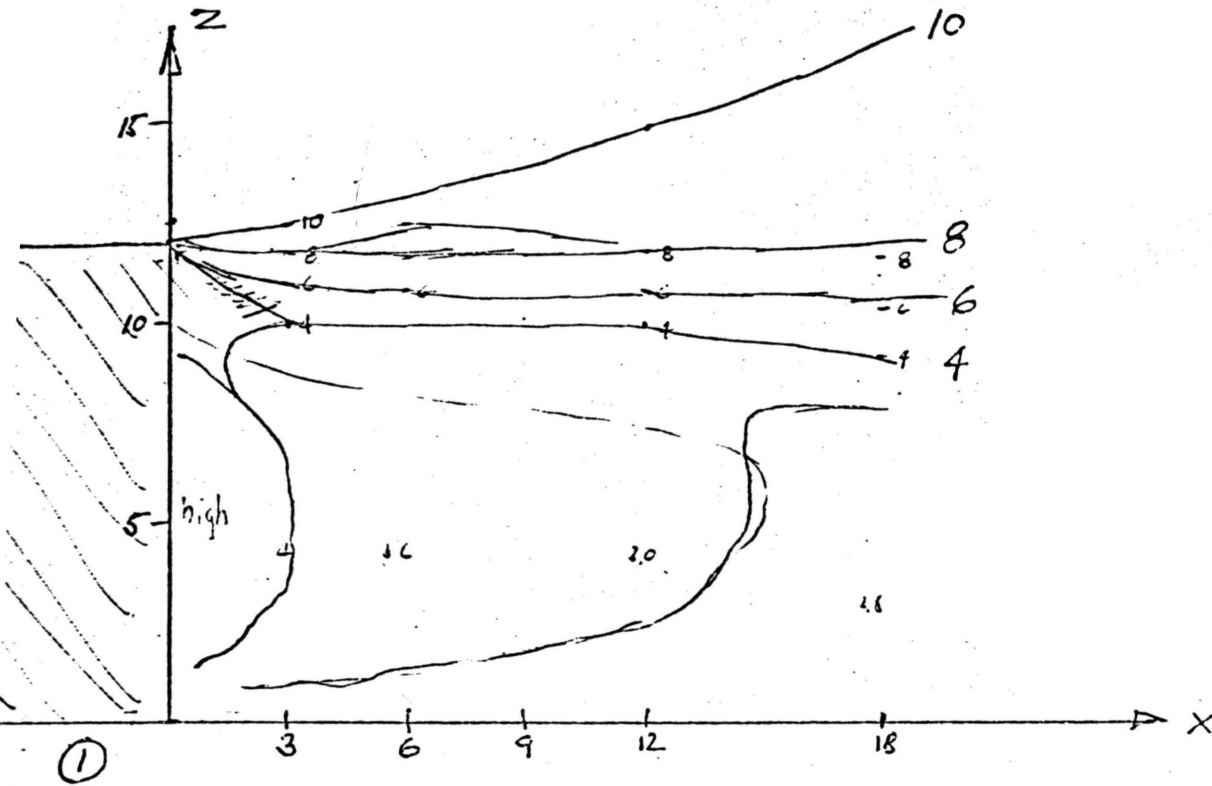
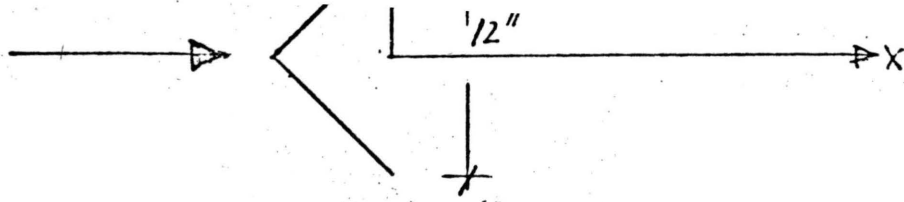
ORIGINAL FILE



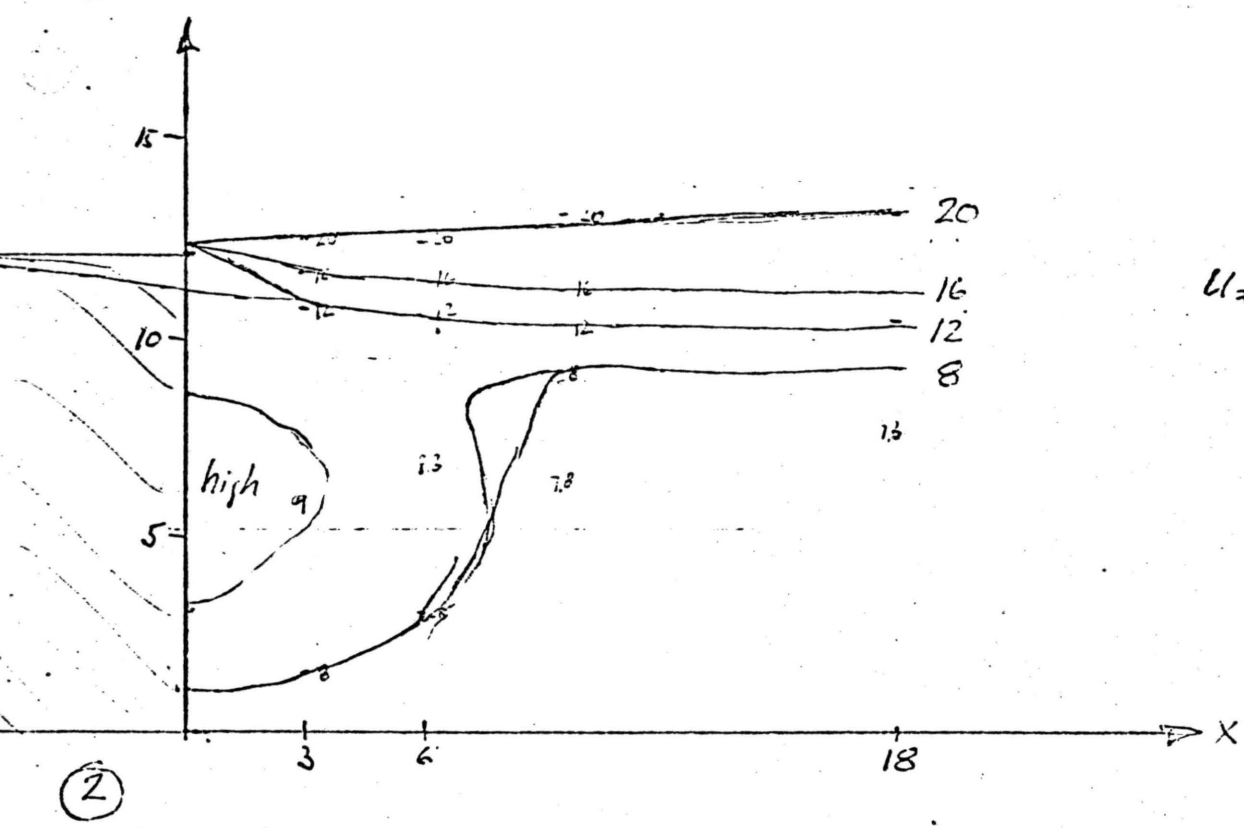
CROSS SECTIONS FOR  $u_{\infty} = 30 \text{ fps}$

Fig. 4

WEDGE



$U_{\infty} = 10$  fps



$U_{\infty} = 20$  fps

VELOCITY AT  $y=0$  ( $\phi$ )

Fig. 5

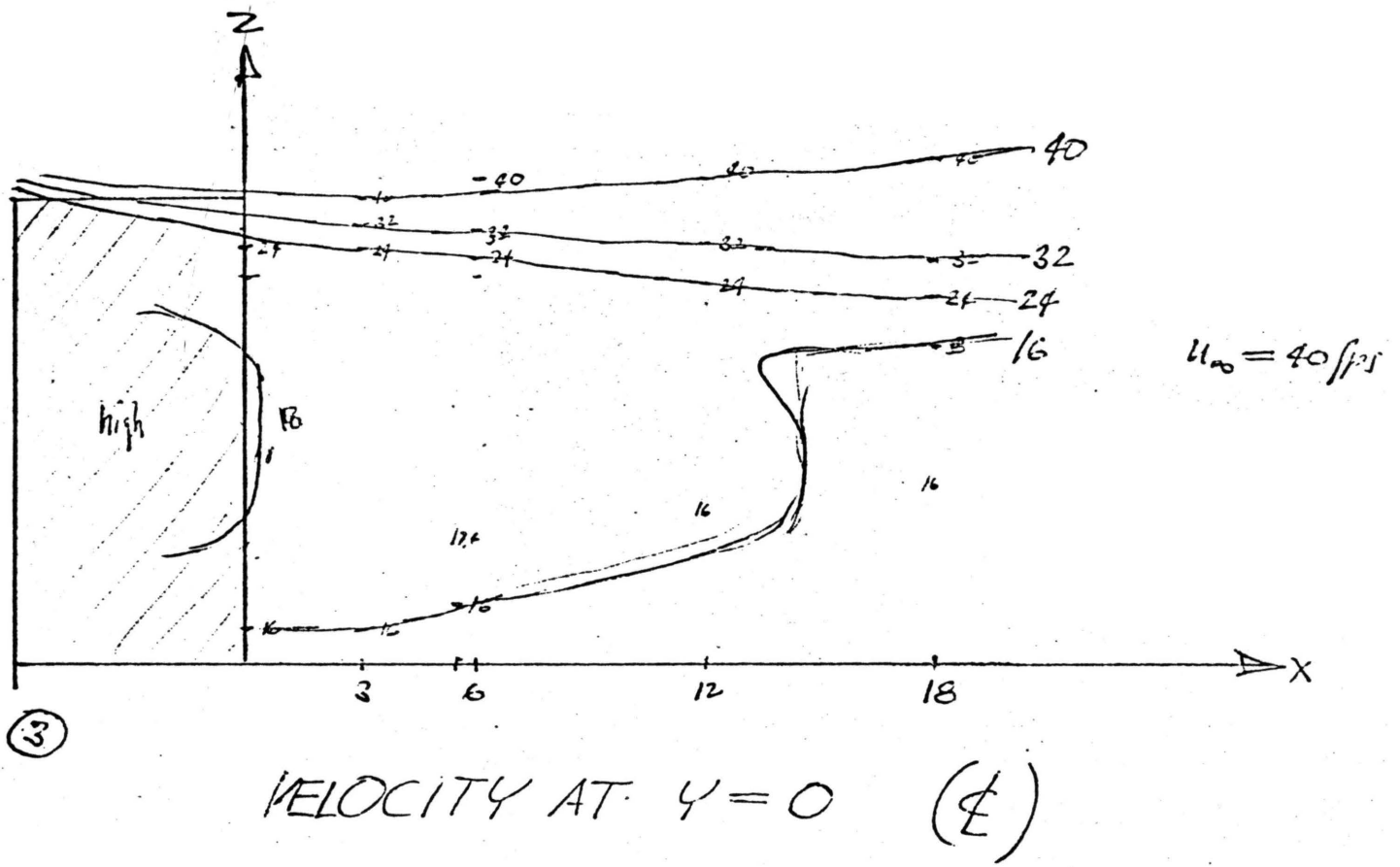
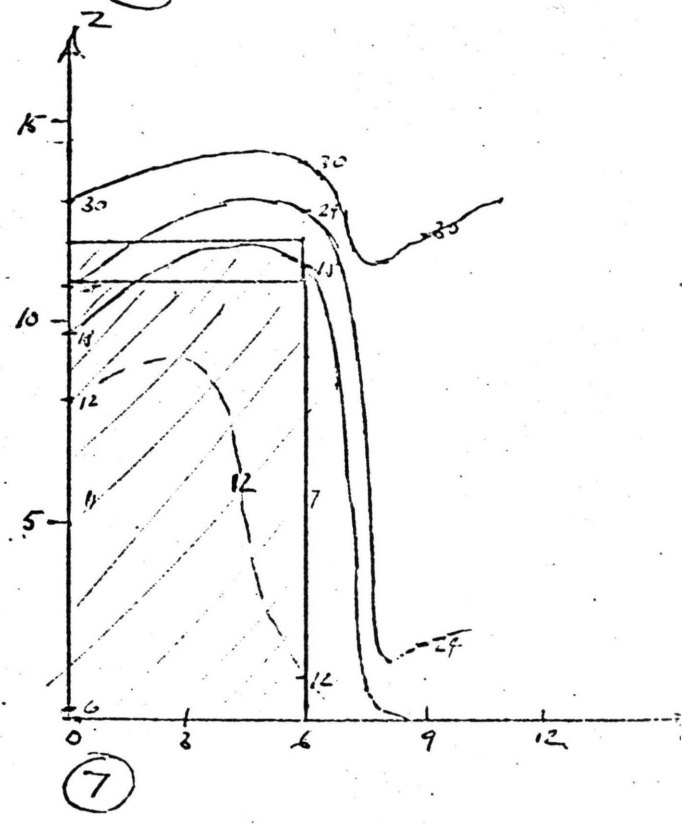
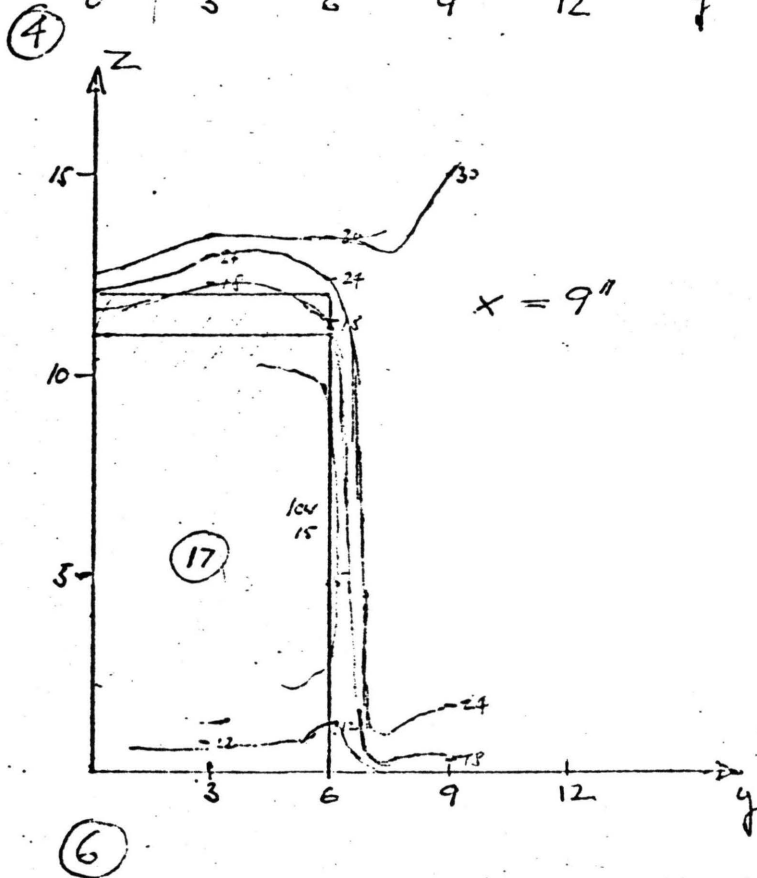
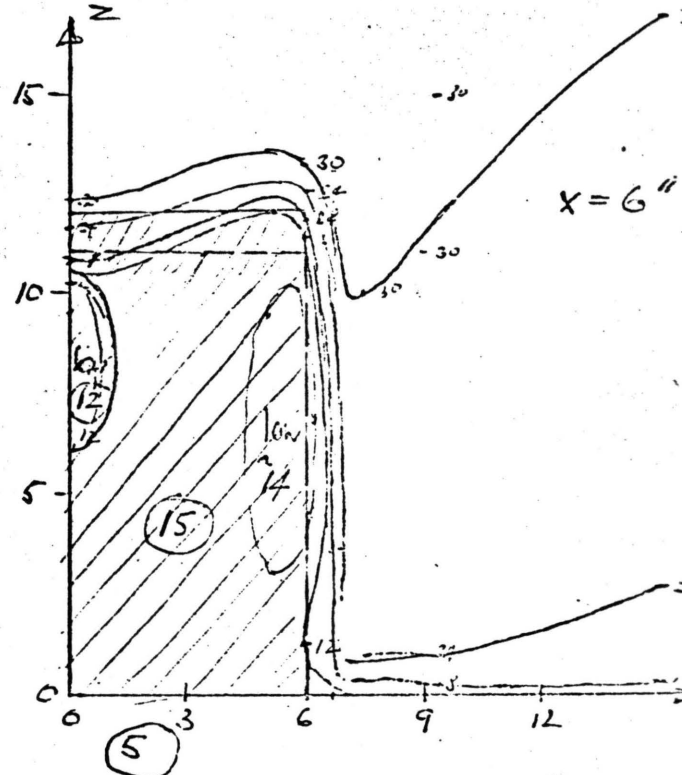
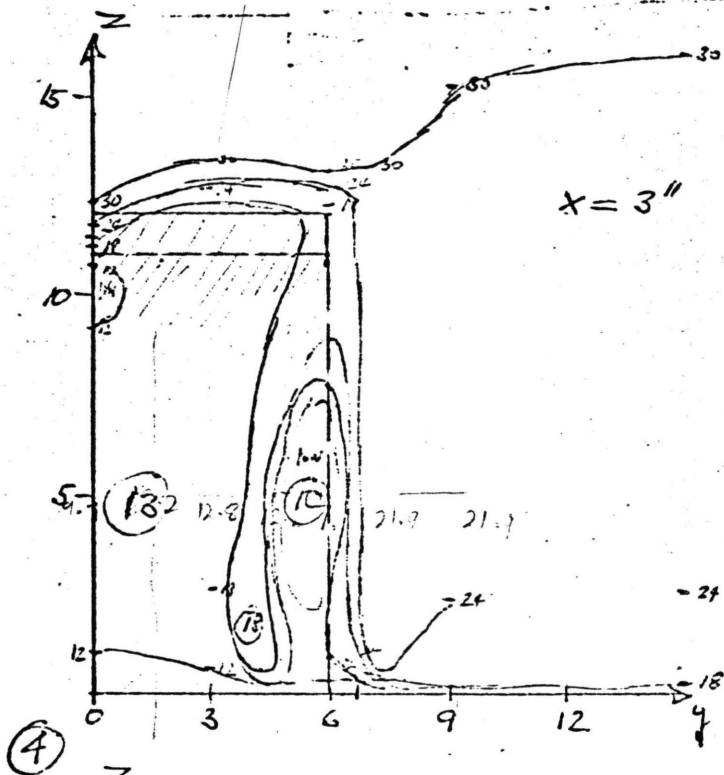
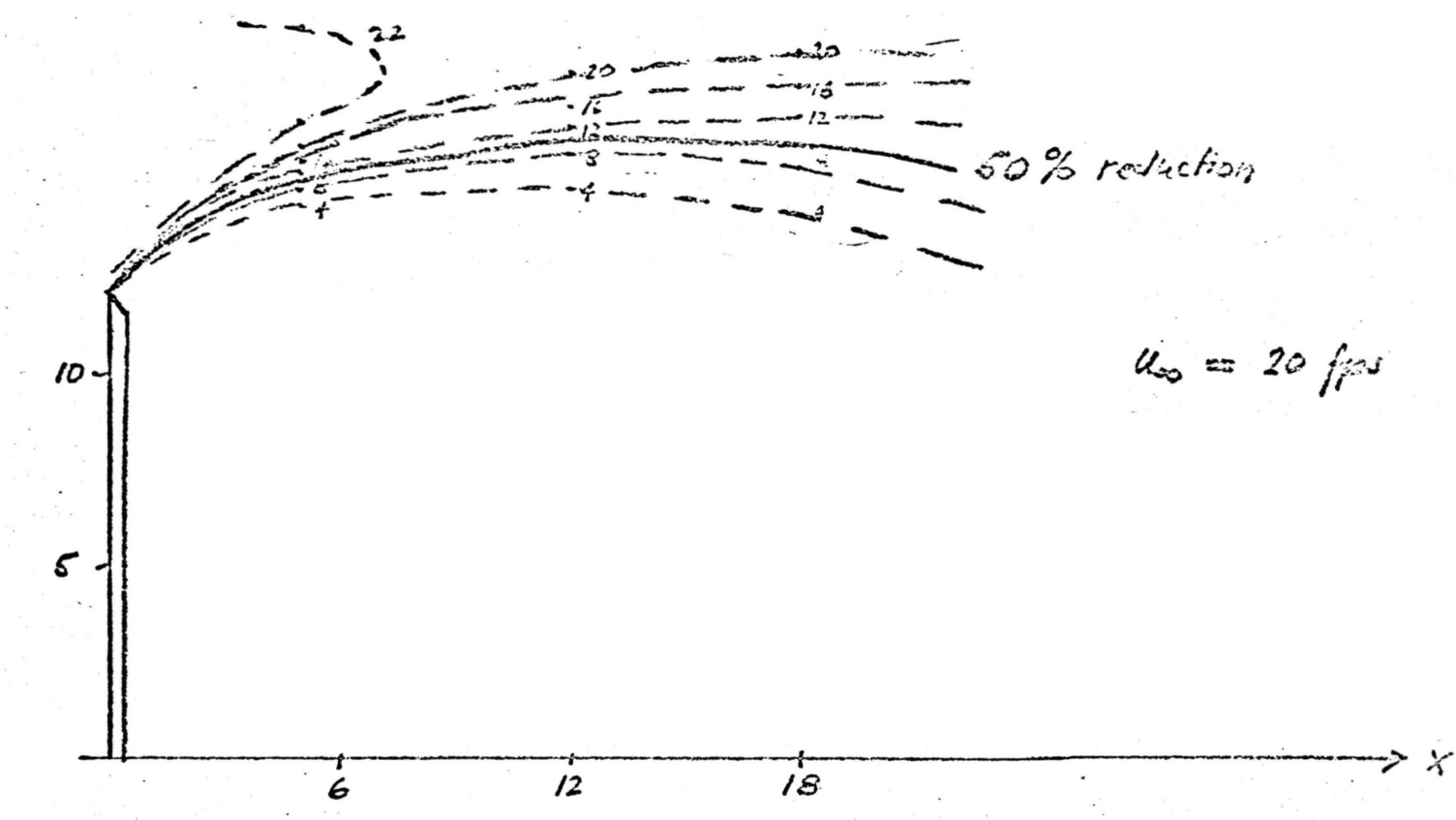
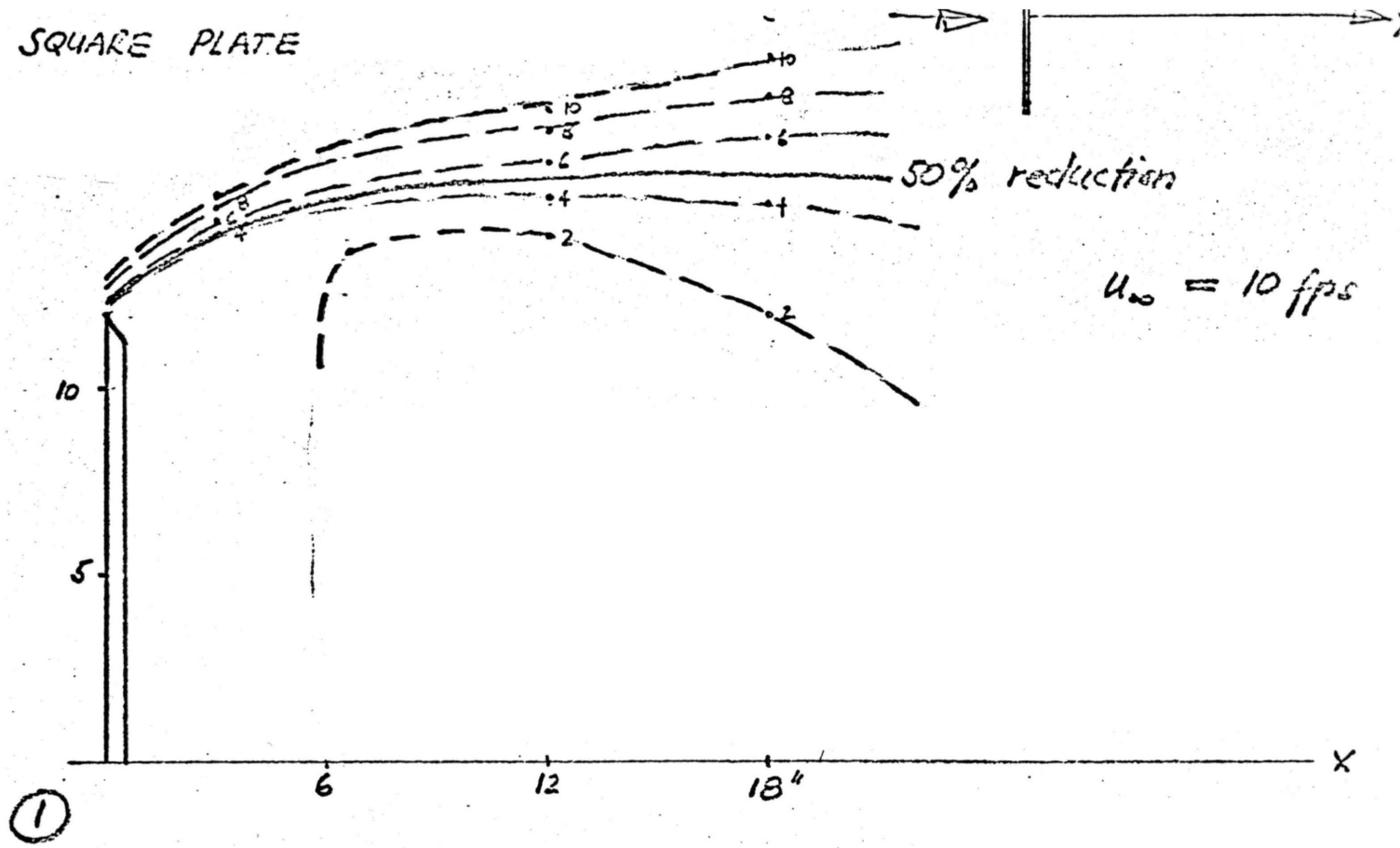


Fig. 6



CROSS SECTIONS FOR  $u_{\infty} = 30 \text{ fps}$   
Fig. 7

SQUARE PLATE

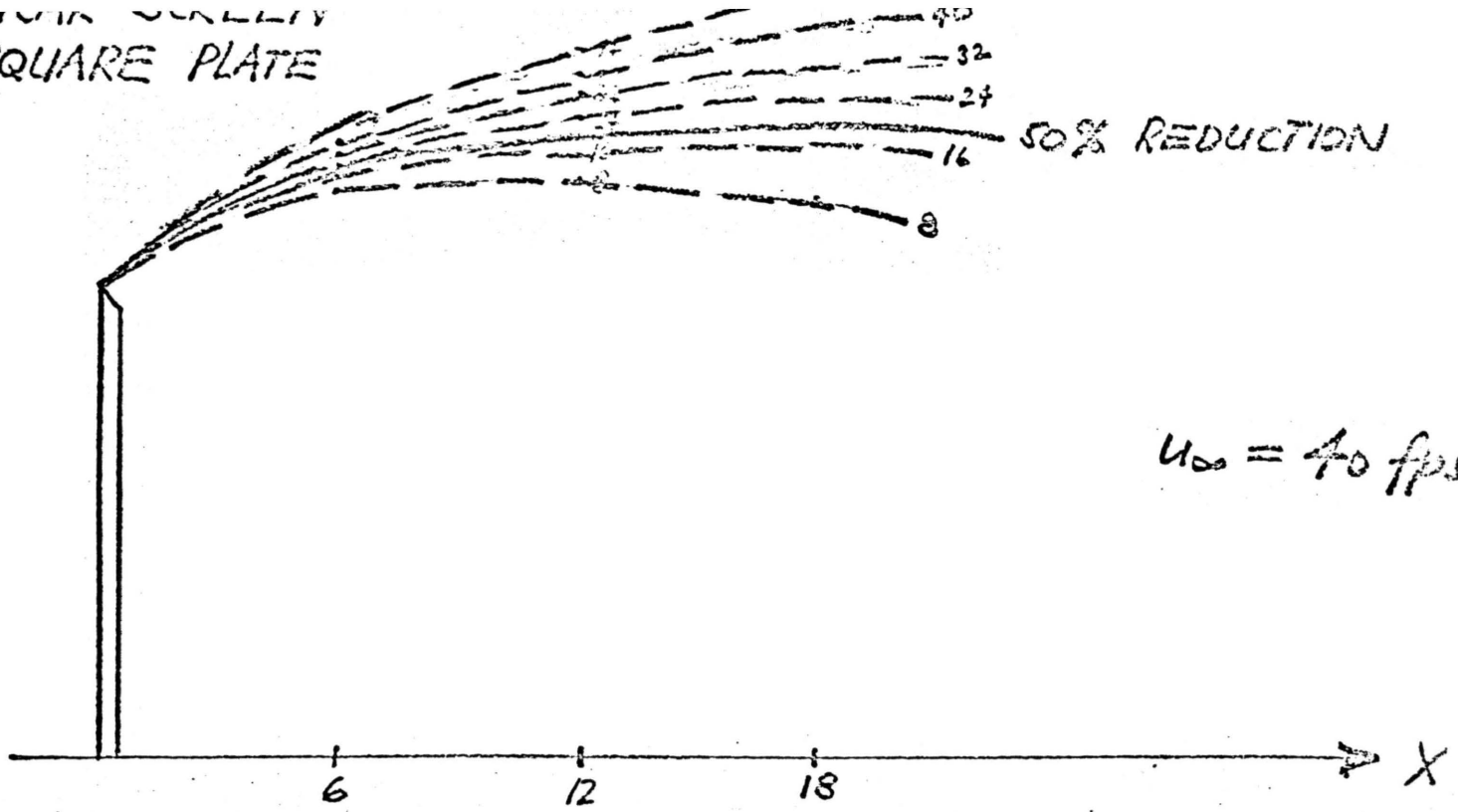


②

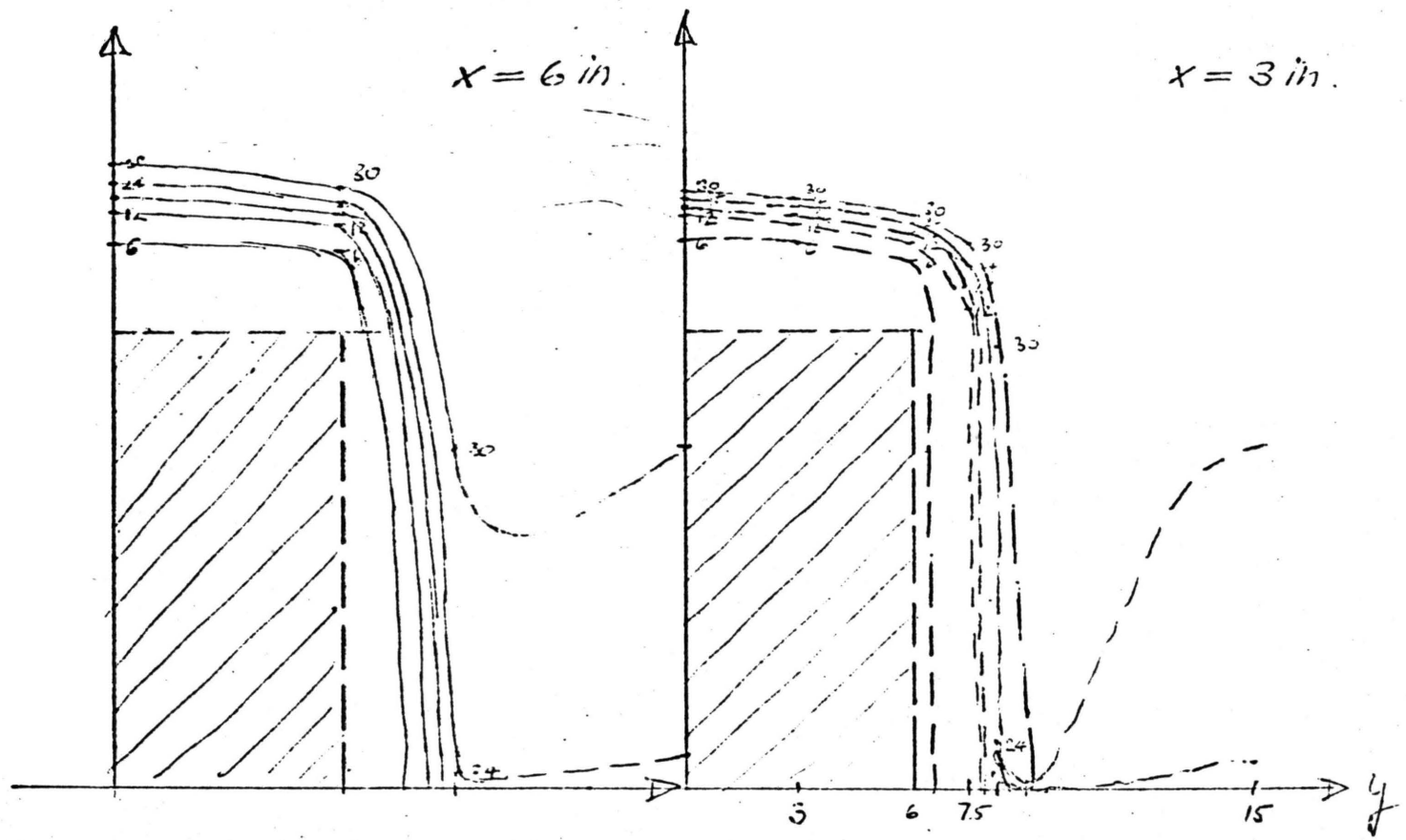
VELOCITY AT  $y = 0$  (ft)

Fig. 8

SQUARE PLATE



③

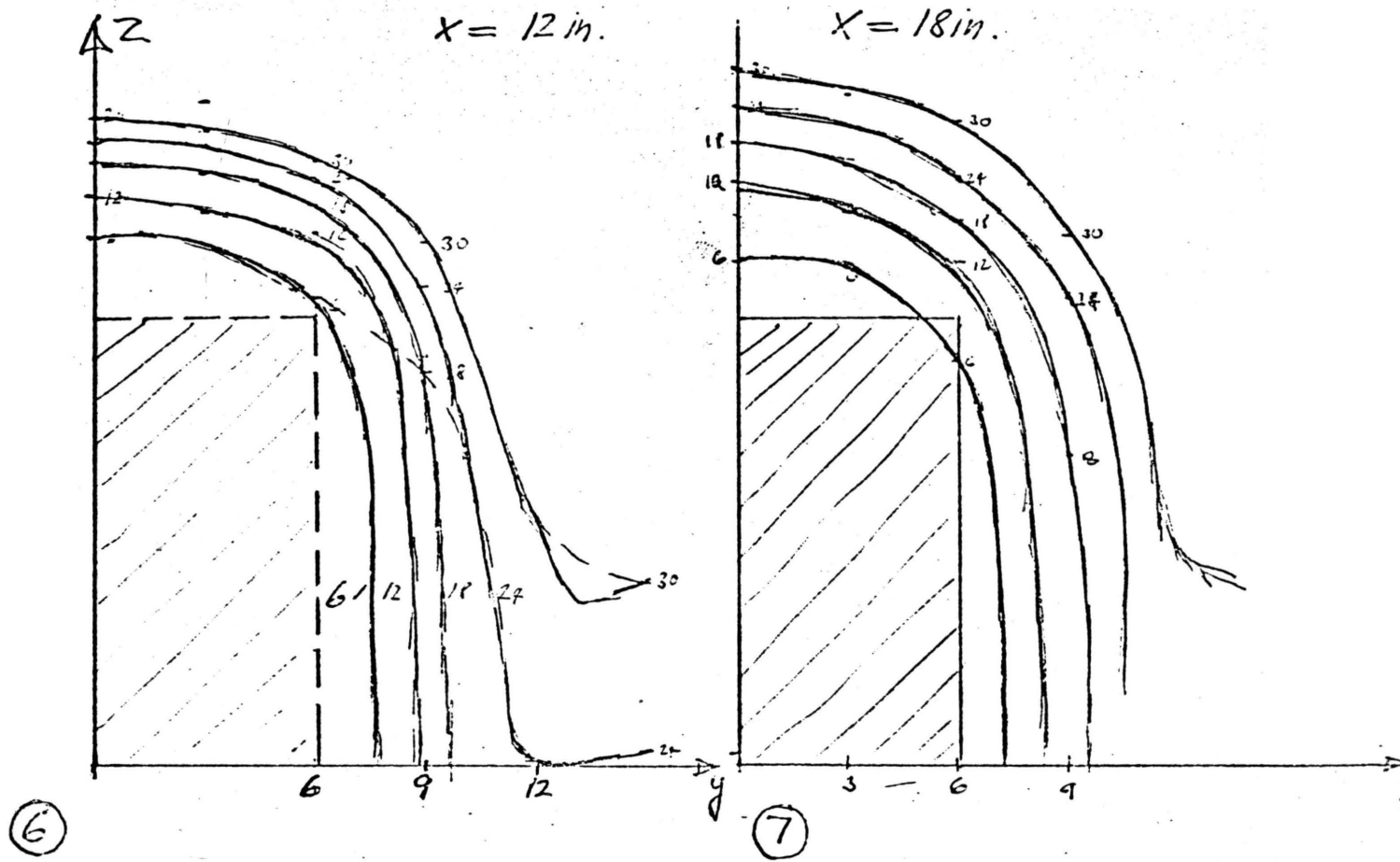


⑤

④

CROSS SECTIONS AT  $U_{\infty} = 30 \text{ fps}$   
Fig. 9

IVAK SCREEN  
SQUARE PLATE

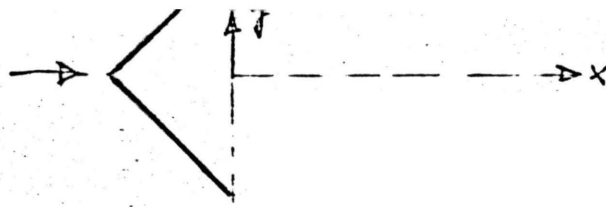


CROSS SECTIONS FOR  $U_{\infty} = 30$  fps.

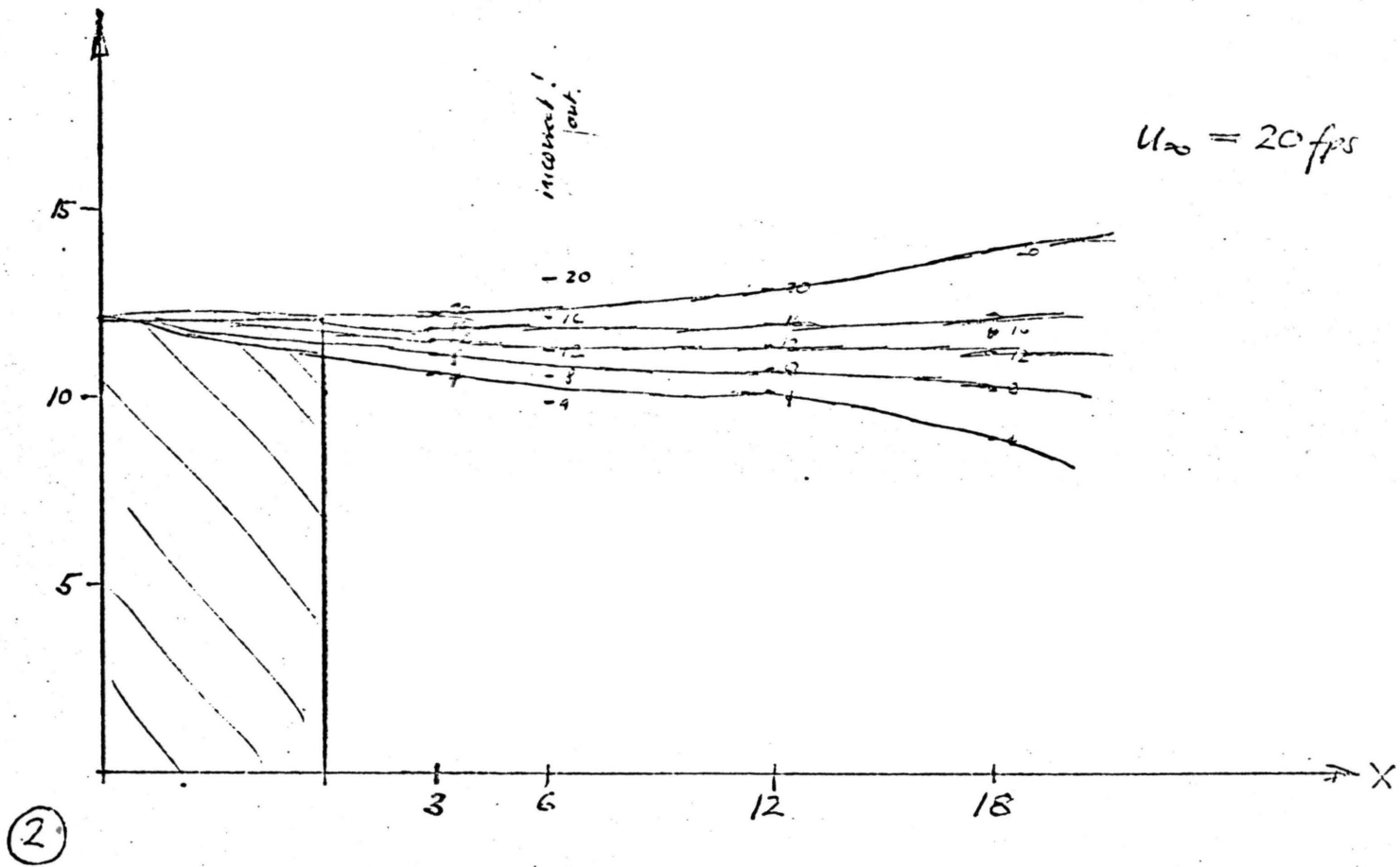
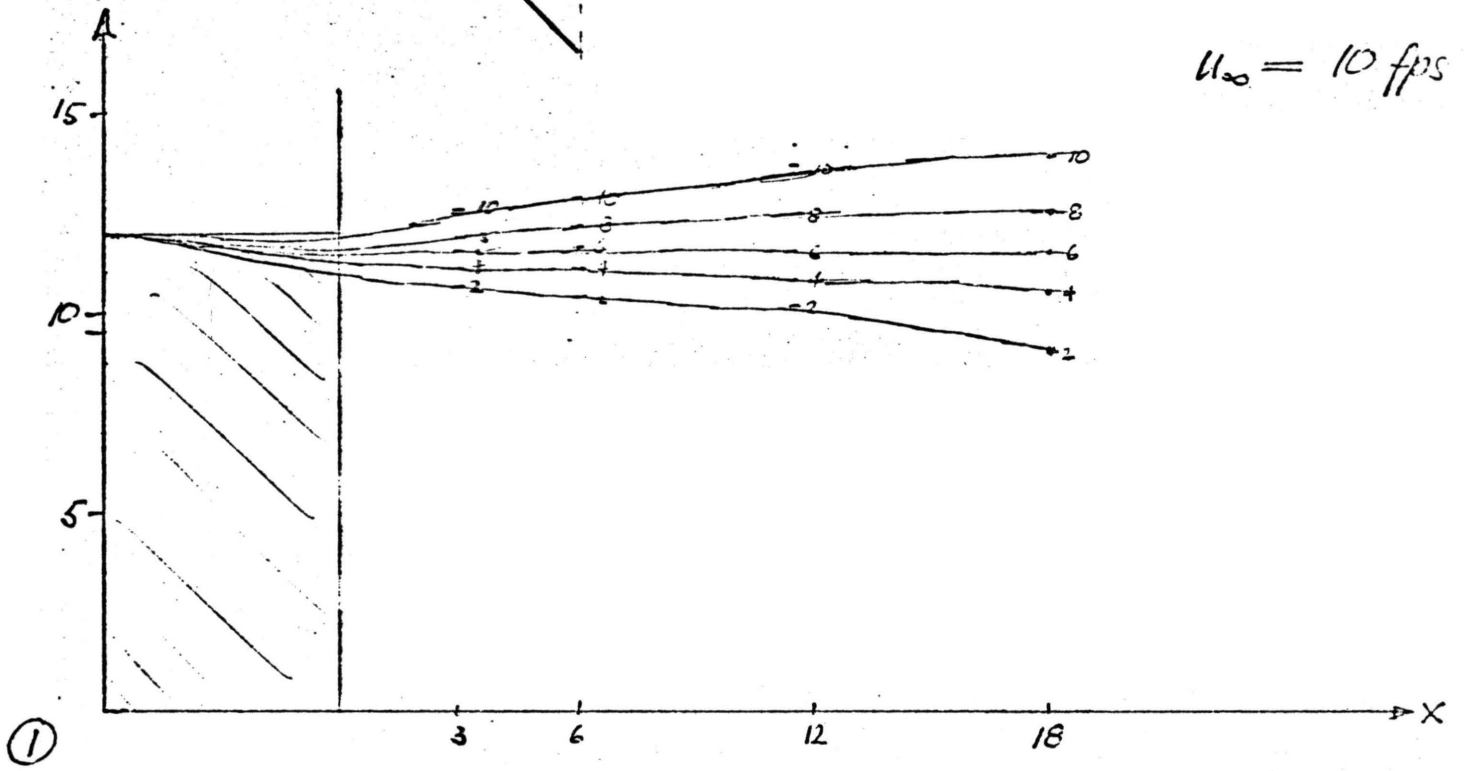
Fig. 10



NOSE SCREEN  
WEDGE



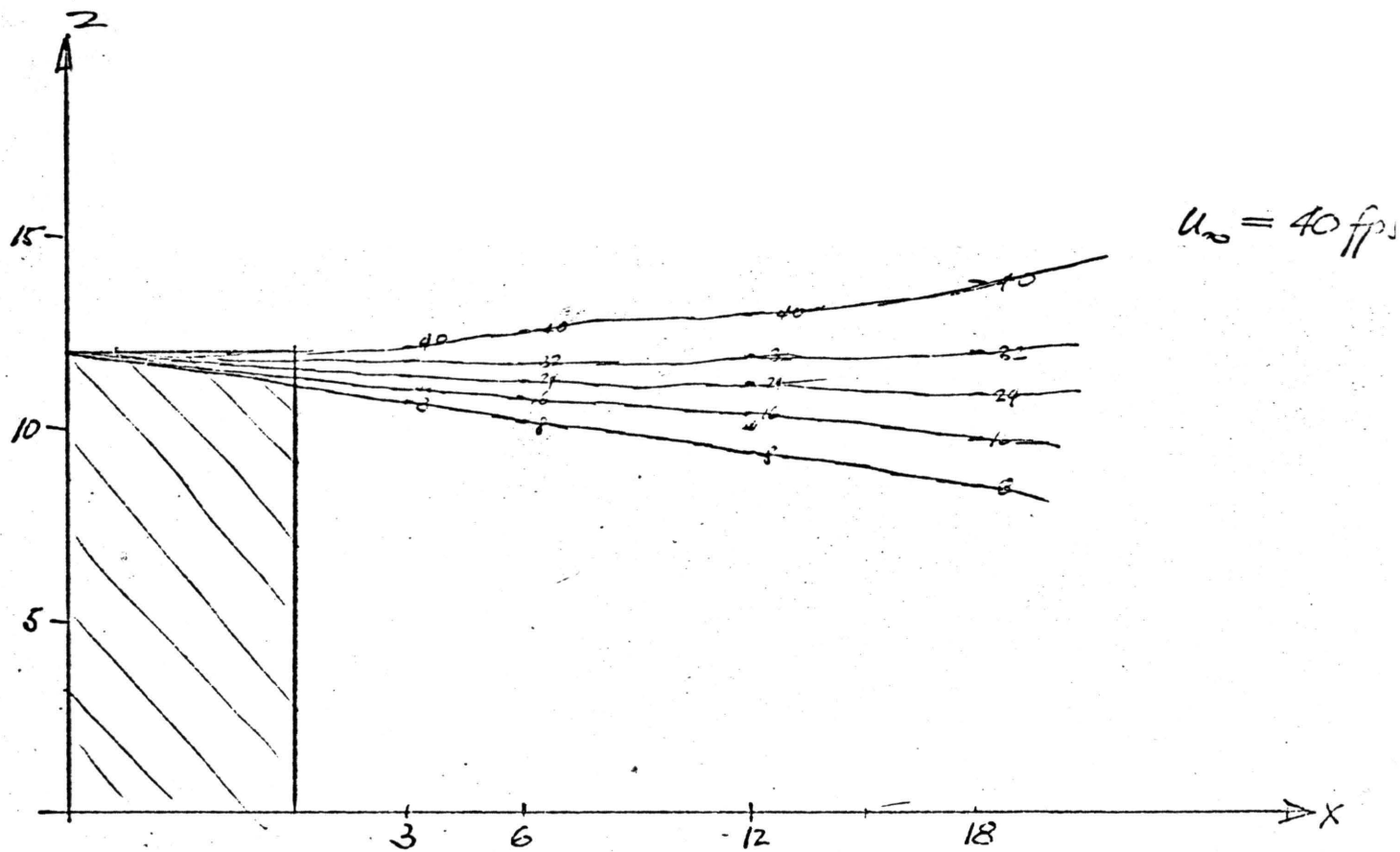
$U_{\infty} = 10 \text{ fps}$



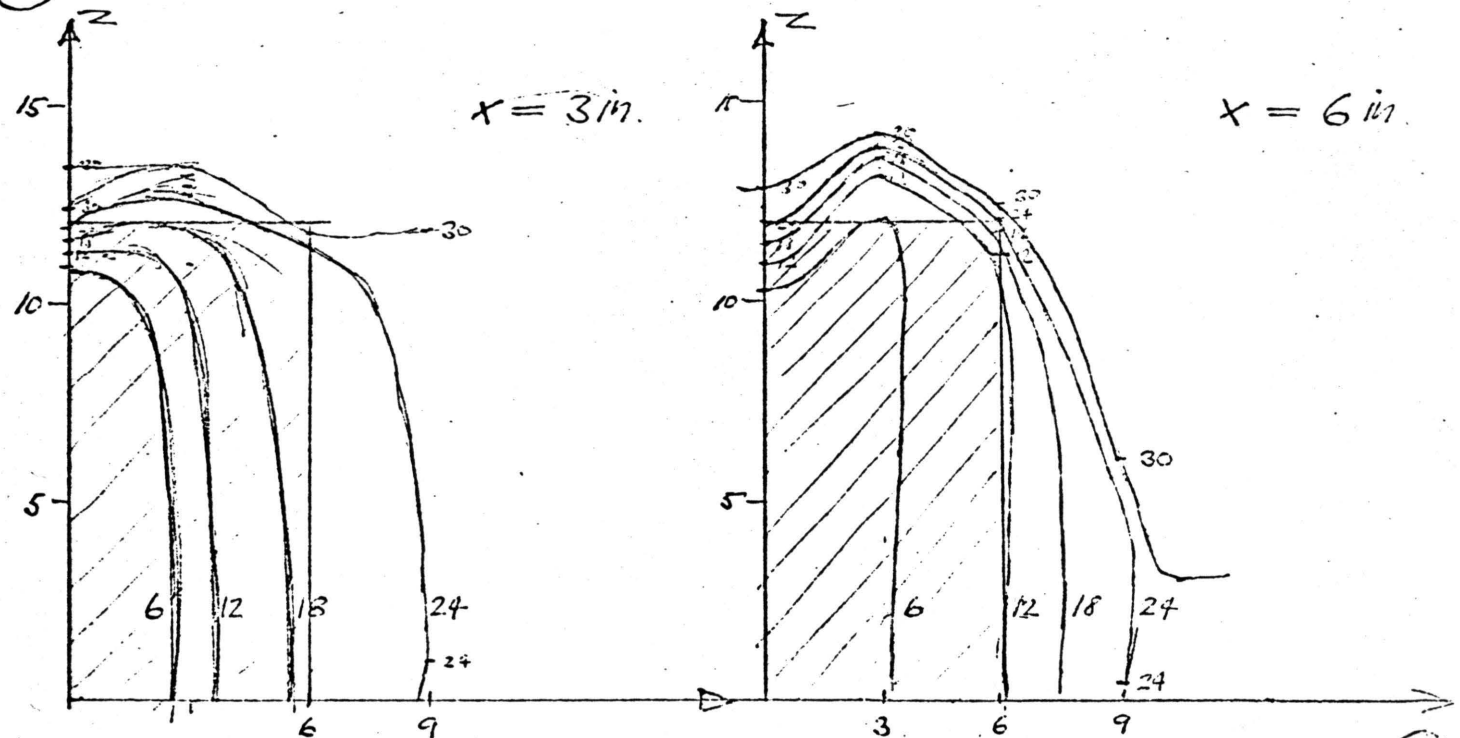
VELOCITY AT  $y=0$  ( $\phi$ )

Fig. 11

IVYAK SCREENY  
WEDGE



③



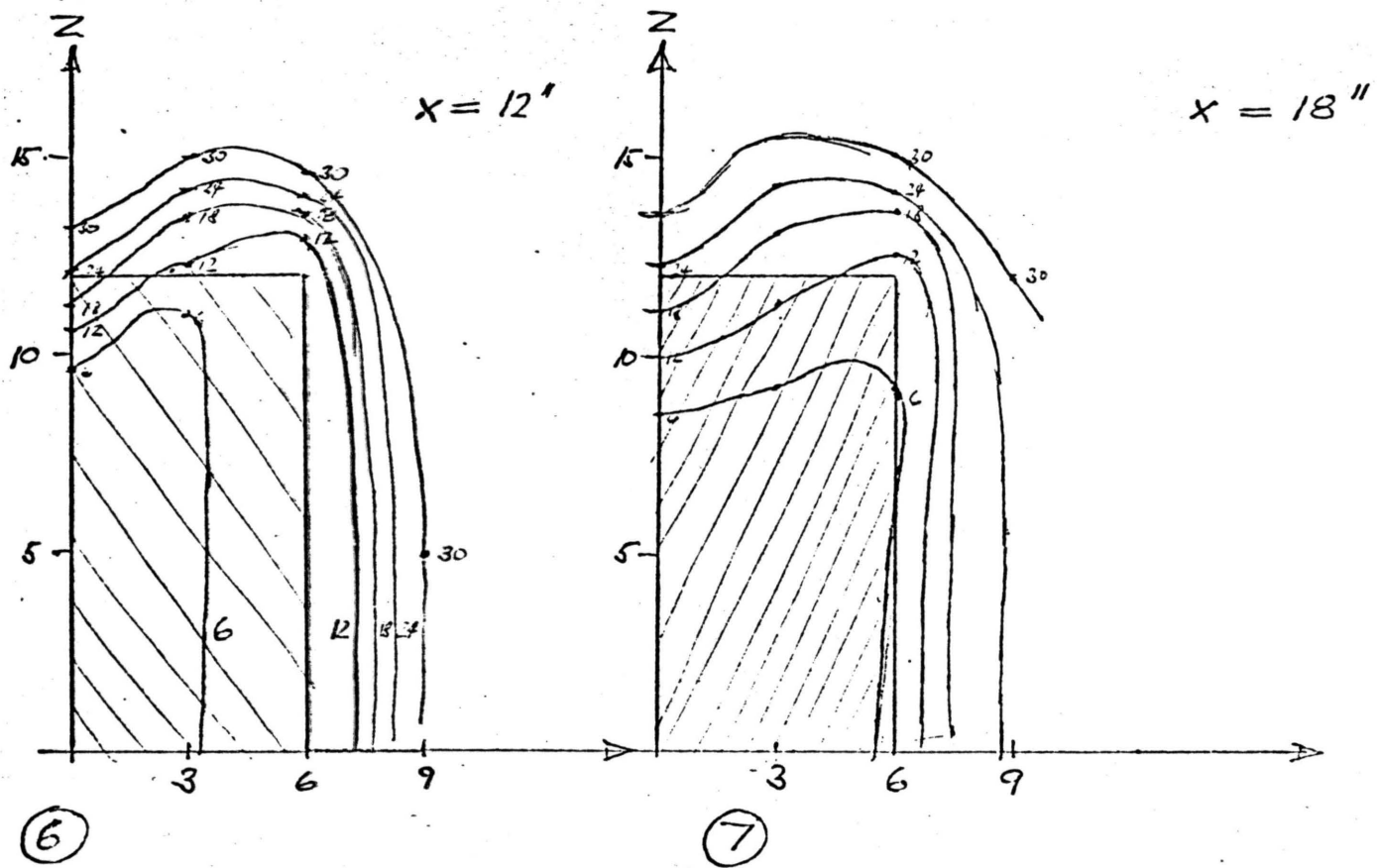
④

CROSS SECTIONS FOR  $u_{\infty} = 30 \text{ fps.}$

⑤

Fig. 12

NCAR SCREEN  
WEDGE



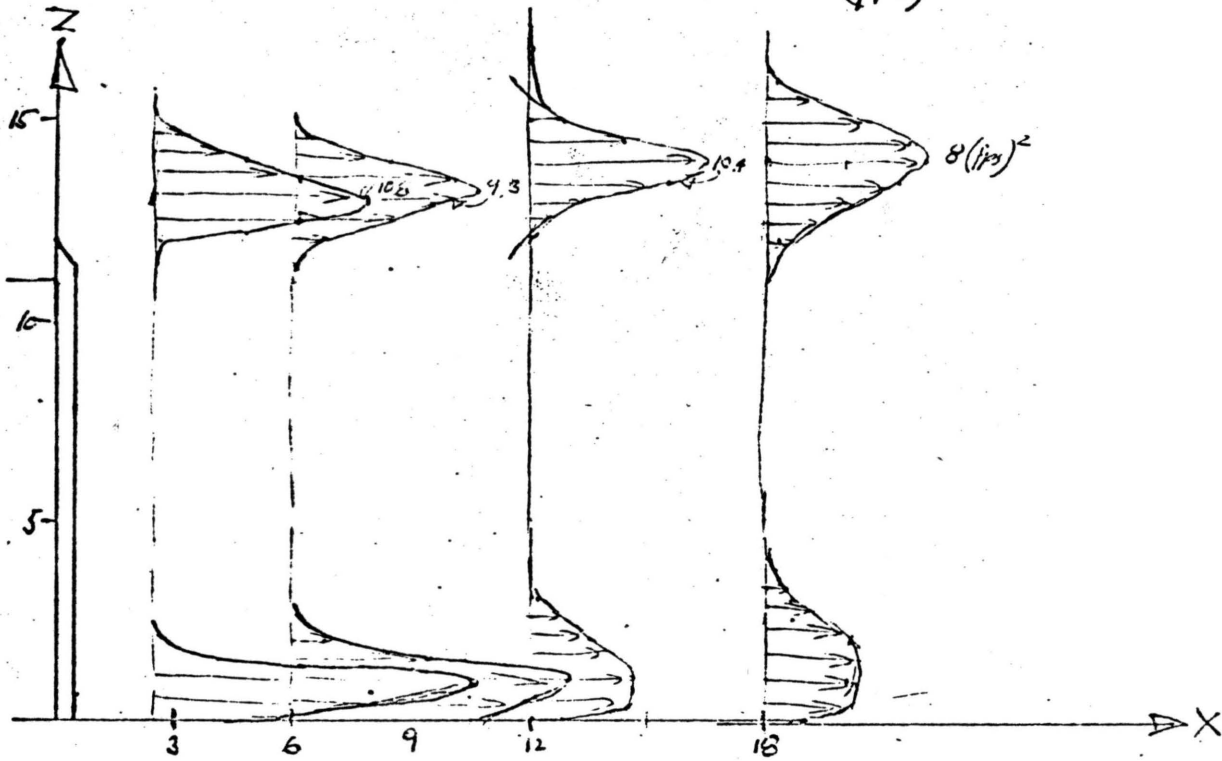
CROSS SECTIONS FOR  $U_{\infty} = 30$  fps.

Fig. 13

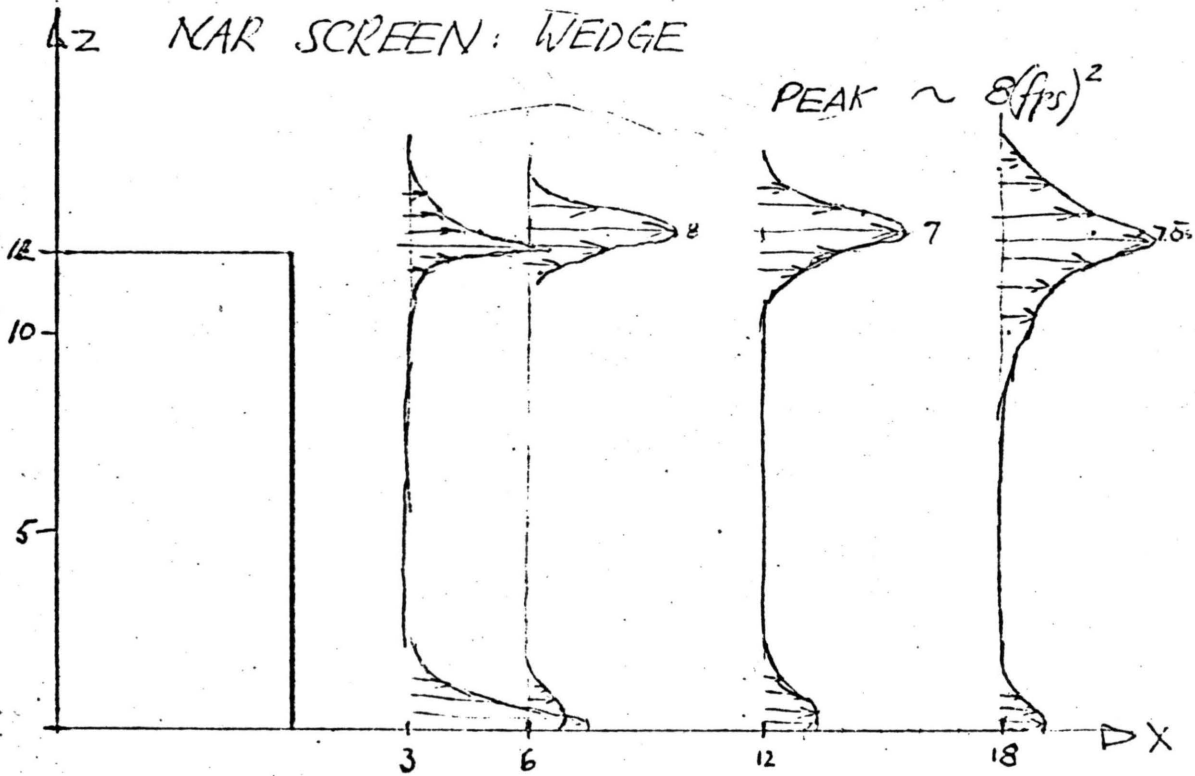
NAR SCREEN  
SQUARE PLATE

BLOCK SCREEN  $\frac{1.4}{2.5} = 0.56$   
NAR SCREEN = 2.2

PEAK:  $11 (fps)^2$



NAR SCREEN: WEDGE



TURBULENT INTENSITY AT  $y = \frac{1}{4}W = 3''$   
 $\overline{u'^2}$

Fig. 14